Intrinsic ordering of quasienergy states for mixed regular/chaotic quantum systems: zeros of the Husimi distribution

1997 J. Phys. A: Math. Gen. 30 1763

(http://iopscience.iop.org/0305-4470/30/5/036)

J. Phys. A: Math. Gen. **30** (1997) 1763–1773. Printed in the UK PII: S0305-4470(97)76145-6

Intrinsic ordering of quasienergy states for mixed regular/chaotic quantum systems: zeros of the Husimi distribution

H Wiescher and H J Korsch†

Fachbereich Physik, Universität Kaiserslautern, D-67653 Kaiserslautern, Germany

Received 5 July 1996

Abstract. A method is proposed which allows an intrinsic ordering of the quasienergy states for a time-periodic quantum system according to the number of essential zeros of the Husimi distribution in phase space. The corresponding classical system shows a typical mixed dynamics with coexisting regular and chaotic regions in phase space. The ordering of states allows a straightforward comparison with semiclassical quantities. Moreover, a direct connection of the organization of zeros with the underlying classical phase space dynamics is demonstrated.

1. Introduction

Generically, a classical system shows an intimate mixture of regular and chaotic dynamics, the well known Poincaré scenario. The corresponding quantum behaviour is much less understood. For the case of an integrable system, a semiclassical EBK quantization can be successfully applied [1–3]. Purely chaotic systems are semiclassically analysed in terms of periodic orbit quantization (see, for example, [4]). Of much recent interest is the connection between classical phase space structures for mixed systems, where regular and chaotic phase space regions are coexistent. Classically, an analysis of the dynamics is greatly simplified by means of a Poincaré section of phase space.

An analysis of individual quantum states by means of quantum representations in phase space, e.g. the Wigner or Husimi densities, allows a direct comparison with classical dynamics (see, for example, [5]). The so-called 'strong' structures (the large density regions) of these distributions show a close relationship to classical phase space structures for one-dimensional time-periodic systems (discrete mappings [6, 7] or continuously driven systems [2, 5, 8–10] also in context with tunnelling through dynamical barriers [11–16]) or two-dimensional time-dependent ones as, for example, the diamagnetic hydrogen atom [17–19].

It has also been shown that a quantum phase space entropy derived from the Husimi density provides a measure of global phase space localization properties, which allows a direct comparison with the corresponding classical quantity [20].

Of recent interest are the 'weak' structures of the quantum phase space densities as, for example, the region of negative values of the Wigner function and the zeros of the Husimi function. Lebœuf and Voros [21] observed marked differences of the arrangement of the zeros of the Husimi density for regular or chaotic regions of phase space, where the zeros are organized on smooth curves in the regular region or they fill the chaotic regions like a

† E-mail address: korsch@physik.uni-kl.de

0305-4470/97/051763+11$19.50

gas. This behaviour was supported by an analysis of the properties of random states in terms of the zeros of random analytic functions (random polynomials) [22, 23]. The *dynamics* of the zeros was analysed by Lebœuf [24] and Cibils *et al* [25] studied the distributions of zeros for the spin-boson model. The problem of phase retrieval in relation to the origin of irreversibility was addressed by [26]. Recently, Dando and Monteiro [17] studied the distribution of zeros for the eigenstates of the diamagnetic Kepler problem and confirmed the observations of Lebœuf and Voros [21], as well as Tualle and Voros [27] in a study of the elliptic and the stadium billiard. The last authors also introduced the idea of using the number of the 'essential' zeros of the Husimi function as a kind of 'fuzzy quantum number'. Very recently, in an impressive study, Prosen [28] reported and analysed the distribution of *many* zeros for a generic but simple two-dimensional time-independent Hamiltonian and demonstrated the uniform distribution on the chaotic region as well as their cubic nearest-neighbour repulsion. The numerical study by Arranz *et al* [29] of a molecular system modelling LiCN supported the idea of using the Husimi zeros as an indicator of regularity or chaoticity.

Clearly, the zeros are not only of marginal importance, because they carry the entire quantum information of a state and allow, in principle, a reconstruction of the state from their positions (in addition, some more information is needed in order to determine the exponential coefficients C_0, C_1, C_2 in (5) below). The zeros are, however, infinite in number (with some exceptions, e.g. harmonic oscillator states or systems with compact phase space [21]). In the following, it will be demonstrated that the zeros can be used to establish an intrinsic ordering of the (regular or chaotic) states. This ordering supports a semiclassical analysis in terms of classical phase space structures.

A presentation in phase space is obtained by projecting the wavefunction onto coherent (minimum uncertainty) states

$$\langle x|p,q\rangle = \phi_{p,q}(x) = \left(\frac{s}{\pi\hbar}\right)^{1/4} \exp\left[\frac{-s(x-q)^2}{2\hbar} + \mathrm{i}\frac{p}{\hbar}\left(x-\frac{q}{2}\right)\right] \tag{1}$$

with mean values q and p for position and momentum, respectively, and uncertainties $\Delta p = \sqrt{\hbar s/2}$, $\Delta q = \sqrt{\hbar/2s}$. The squeezing parameter $s = \Delta p/\Delta q$ can be adapted to the problem under investigation. The Husimi density is

$$\varrho(p,q) = \left|\int \phi^*_{p,q}(x)\psi(x)\,\mathrm{d}(x)\right|^2 \tag{2}$$

with normalization

$$\frac{1}{2\pi\hbar}\int \varrho(p,q)\,\mathrm{d}p\,\mathrm{d}q = 1. \tag{3}$$

A representation in the complex $z = (sq + \mathrm{i}p)/\sqrt{2s\hbar}$ plane, $|z\rangle = |p,q\rangle$, reveals the analytic properties: the Bargmann [30] transform $\langle z|\psi\rangle$ is determined by an entire function $F(z)$ of order $\leqslant 2$,

$$\langle z|\psi\rangle = \exp(-\tfrac{1}{2}|z|^2)F(z^*) \tag{4}$$

where $F(z)$ can be expressed by the Weierstrass–Hadamard factorization in terms of the zeros $z_1, z_2, \ldots$ and the m-fold zero at the origin,

$$F(z) = z^m \mathrm{e}^{C_0+C_1z+C_2z^2}\prod_n \left(1-\frac{z}{z_n}\right)\exp\left[\frac{z}{z_n}+\frac{1}{2}\left(\frac{z}{z_n}\right)^2\right]. \tag{5}$$

Hence the Husimi density $|\langle z|\psi\rangle|^2$ is uniquely determined by its zeros and the three coefficients C_0, C_1, C_2, where C_0 takes care of the normalization, and C_1, C_2 are related to translation, rotation and squeezing in phase space.

It can be shown that the class of states with a *finite* number of zeros in the z-plane is very much restricted and consists only of generalized harmonic oscillator states [31]. Generally, we find an infinite number of zeros, most of which are, however, far away in the complex plane, i.e. in regions where the density is extremely small. Here we confine ourselves to an investigation of the nearby zeros. We hope to demonstrate that the skeleton of the zeros provides a useful and interesting insight into the quantum phase space organization.

2. Dynamics of a periodically driven anharmonic oscillator

As an example for a system with mixed regular and chaotic behaviour, we consider a forced quartic oscillator

$$H(p,q,t) = \frac{p^2}{2m} + bq^4 - fq\cos(\omega t) \tag{6}$$

which is time-periodic with period $T = 2\pi/\omega$. We choose parameter values $b = 0.25$, $f = 0.5$, $\omega = 1$, a case for which the classical-quantum correspondence [9, 32] and the semiclassical EBK quantization of the quasienergy states

$$\langle q|\alpha\rangle = \psi_\alpha(q,t) = \mathrm{e}^{\mathrm{i}\epsilon_\alpha t/\hbar}u_\alpha(q,t) \qquad u_\alpha(q,t+T) = u_\alpha(q,t) \tag{7}$$

have been investigated recently [2]. A value of $\hbar = 0.05$ is used in the quantum computations presented here, which are obtained by time propagation of wavefunctions on a grid followed by a spectral method for extracting the quasienergy ϵ_α and the quasienergy states (for more details see [33, 34]). It should be stressed that (7) defines the quasienergies ϵ_α only up to integer multiples $\hbar\omega$. Moreover, the ordering of the ϵ_α—or the quasiangles $\theta_\alpha = \epsilon_\alpha T/\hbar$—is arbitrary, in contrast to the time-independent case, where the states can be unambiguously ordered by the energy eigenvalues. In previous studies, the states have been ordered by increasing expectation values of, for example, the kinetic energy or the Hamiltonian at time zero [2, 3, 9, 35]. Evidently, such an ordering reflects the phase space morphology only in a very crude manner and states with a neighbouring quantum number α may have a very different nature. Moreover, it is almost impossible to detect missing states in a given sequence. An alternative ordering scheme is provided by the zeros of the Husimi distribution, whose pattern clearly reflects the classical phase space organization.

For the Hamiltonian (6), the classical dynamics determined by the canonical equations of motion shows the characteristic mixture of regular and chaotic motion. This is most conveniently displayed by means of a Poincaré section of phase space. Figure 1 shows a stroboscopic plot of the trajectory at times $t_n = nT$, $n = 0, 1, 2\ldots$ for selected initial conditions. There is a clear division of phase space into three different regions: a chaotic region is sharply separated from an outer regular region†. A second regular region is centred on a T-periodic trajectory and appears as a stability island embedded in the chaotic sea. The phase space area of the inner island is $\oint p\,\mathrm{d}q = 2.25$ and the chaotic sea covers an area of $\oint p\,\mathrm{d}q = 7.85$.

In quantum mechanics, one can compute the time dependence of a minimum uncertainty state (1) initially centred at (p_0, q_0) and the corresponding time-dependent Husimi density

† Note that for the Hamiltonian (6) all classical trajectories are bounded by invariant curves as proven, e.g. in [36].

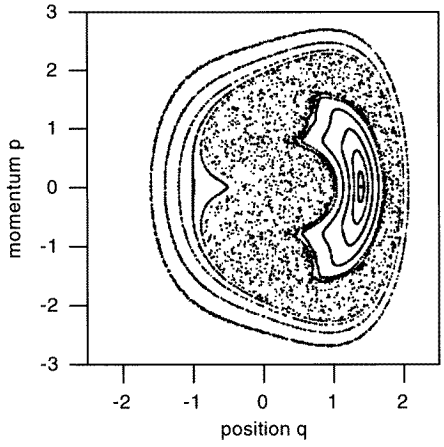

Figure 1. Classical stroboscopic Poincaré section for a driven quartic oscillator (parameters $b = 0.25, f = 0.5$, $\omega = 1$).

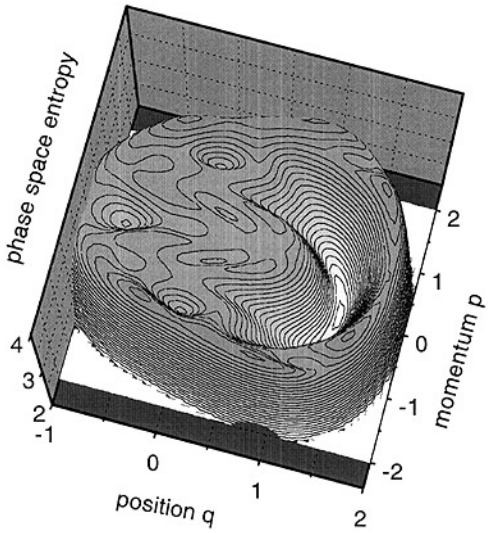

Figure 2. Quantum phase space entropy for the quantum system corresponding to figure 1.

at times $t_n = nT$

$$\varrho(p, q; p_0, q_0; t_n) = \langle p, q|U(t_n)|p_0, q_0\rangle = \int \phi^*_{p,q}(x)\psi_{p_0,q_0}(x, t_n)\,\mathrm{d}x \tag{8}$$

(we use a squeezing parameter $s = 1$). The global phase space structure can be obtained by calculating the quantum phase space entropy as a measure of the (time averaged) spreading of the wavepacket [20]. If the Husimi distributions (2) of the individual quasienergy states are known, the time averaging reduces to the computation of an averaged Husimi distribution (assuming nondegenerate quasienergies):

$$\bar{\varrho}(p, q; p_0, q_0) = \lim_{N\to\infty} \frac{1}{N+1} \sum_{n=0}^{N} \varrho(p, q; p_0, q_0; t_n) = \sum_{\alpha} \varrho_\alpha(p, q)\varrho_\alpha(p_0, q_0) \tag{9}$$

and the phase space entropy is then given by

$$S(p_0, q_0) = -\frac{1}{2\pi\hbar} \int \bar{\varrho}(p, q, p_0, q_0) \ln \bar{\varrho}(p, q, p_0, q_0)\,\mathrm{d}p\,\mathrm{d}q. \tag{10}$$

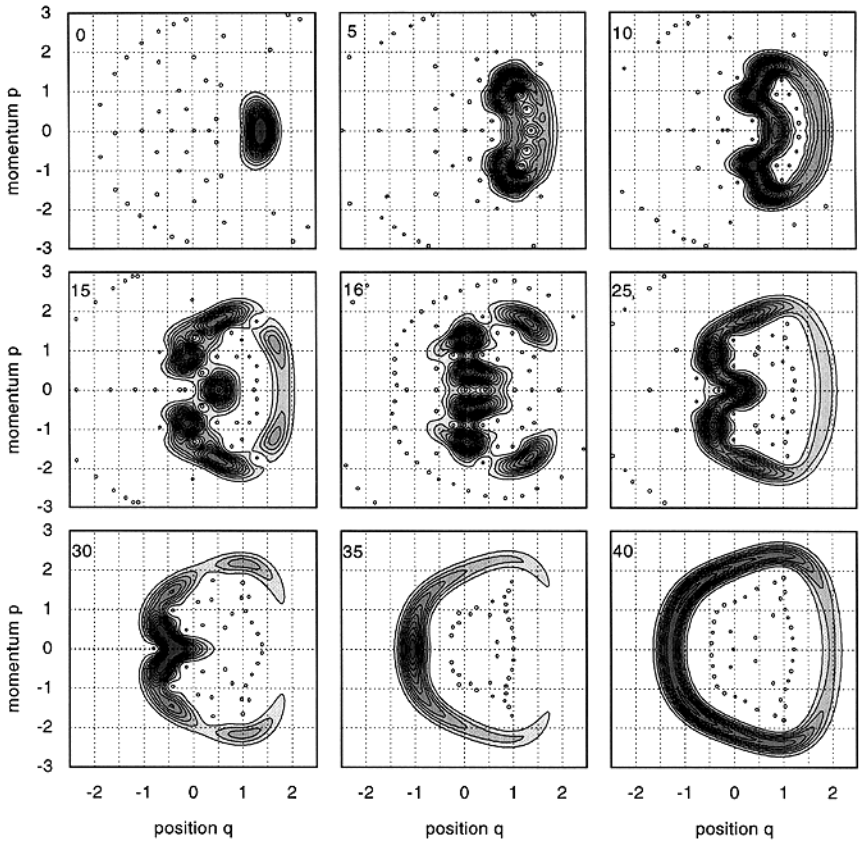

Figure 3. Husimi distributions of selected quasienergy states (dark colours represent high densities). The number in each diagram is the ordering number assigned according to the zeros of the distributions (marked by open circles).

The quasienergy states of the quartic oscillator (6) have been determined numerically for $\overline{h} = 0.05$†. From the Weyl rule, we expect seven states localized on the stability island and 25 states supported by the chaotic region. Figure 2 shows the phase space entropy of the quantized system (6). The stability island appears as a region with low entropy values. It is embedded in a high entropy area which corresponds to the classical chaotic region. On average, there is a striking structural agreement with the classical Poincaré section in figure 1. One observes, however, some regions with a considerably lower value of the entropy, i.e. a quantum localization in phase space. This reflected in the properties of the individual quasienergy states, which are discussed in the following.

3. Zeros of the Husimi distributions

The individual quasienergy states $|\alpha\rangle$ can be classified by means of their Husimi distributions, e.g. by computing their overlap with the different classical phase space regions. A selection of the complete catalogue of the Husimi distributions for 'low' quasienergy states is shown in figure 3. The phase space region shown agrees with the region of the

† The precise nature of the quantum quasienergy spectrum for the driven quartic oscillator (6) is still unknown. It has been shown, however, that the spectrum is pure point for small driving amplitude f [37].

classical Poincaré section (1). Dark shading of the contour plot corresponds to regions of large density. The zeros of the distribution are marked by circles. Apparently, the main characteristic feature of the individual Husimi distributions is the strong localization on a classical flux tube. This tube is, of course, to a large extent destroyed in the chaotic region, however, it is still visible in the quantum case as a highly organized sequence of maxima and saddle points. A remarkable result is the possibility of ordering the states according to the number of 'essential' zeros, i.e. those, which appear inside this main ridge of the Husimi distribution. This relation seems to be one to one, at least in the present case, which suggests the use of this ordering number (given in the upper left corner of the graphs) as the α label of the quasienergy states. Infinitely many additional zeros can be found outside, where the density is very small. It should be noted that this numbering appears to be similar to the assignment of a 'fuzzy' quantum number for the case of billiard systems in [27].

The first graph in figure 3 shows the ground state $|0\rangle$ without any zero in the inner region of high density. Additional zeros are distributed almost uniformly over the classically chaotic region of phase space (see figure 1). The zeros at larger distances, i.e. in the region of very small values of the Husimi density, do *not* represent true zeros of the distribution. They are strongly influenced by the finite numerical precision. A fraction of these zeros appear to be distributed along a smooth curve, similar to the crystallization effect discussed for the roots of random polynomials [22]. This behaviour is found for all states. In figure 3, these 'spurious' zeros are not shown for the states 30, 35 and 40.

For the state $|5\rangle$, which is still localized on the island region, we find five zeros inside the main region. For the state $|10\rangle$, the 10 zeros are in a region where the Husimi density is small, surrounded by a region of high density. Using criteria as overlap with the classical regions of phase space or the value of the phase space entropy, this state is classified as belonging to the chaotic part of the phase space. The states 0–6 (ordered according to the zeros) show a strong overlap with the inner stability island, the states 7–31 with the chaotic region, i.e. we have seven states localized on the inner island and 25 states localized on the chaotic region, as predicted by the Weyl rule.

All the essential zeros are still localized in the region of the stability island, but their distance from the period-one fixed point at the centre has increased. The inner region of smaller values of the Husimi density, where the relevant zeros appear, widens with an increasing ordering number up to state $|40\rangle$, which shows a pronounced crater-shaped structure, inside of which the essential zeros are found. This state is classified as an outer regular state.

By closer inspection, two structural transitions can be found for the states $15 \leftrightarrow 16$ and $21 \leftrightarrow 22$. For the state $|15\rangle$, which localized in the stability island, we observe six zeros embedded in the region of high density in addition to the 15 principal zeros, which undergo a resonance transition from $|15\rangle$ to $|16\rangle$ as discussed in detail below. A similar phenomenon is found for the transition $21 \leftrightarrow 22$.

It may also be of interest to point out that the fraction of zeros on the real axis (in particular in the interval in the chaotic region) is quite large, which seems to be typical for symmetry lines (here the real axis) [22].

4. Semiclassical considerations and influence of classical phase space structures

In the regular phase space regions, where a semiclassical quantization is possible, the ordering number assigned by the zeros agrees with the semiclassical quantum number [2, 3]. The present ordering scheme, however, also covers the chaotic region and continues to the outer regular regime. Moreover, this scheme seems to provide a grouping of states into different categories distinguished by their quasienergy spacings.

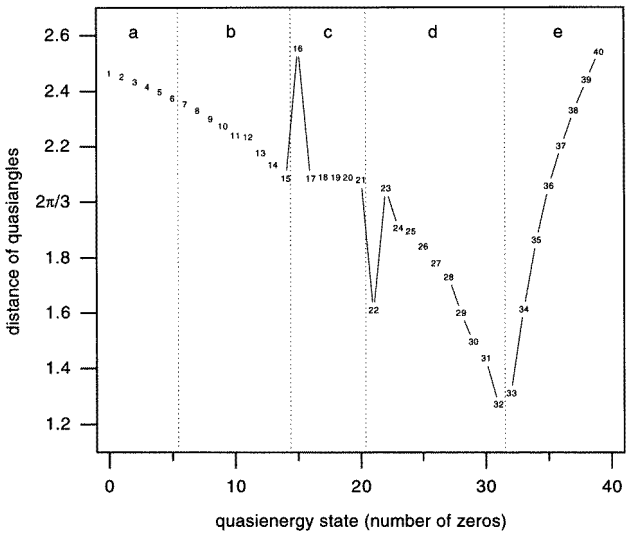

Figure 4. Quasienergy distances as a function of the ordering number. States in (a) are localized in the inner regular region, states (e) in the outer regular region. The chaotic region (b–d) is interrupted by the resonance states (c).

4.1. Quasiangle distance

The ordering of the quasienergy states by their zeros allows a comparison with semiclassical considerations also in the chaotic region of phase space. As a result of the semiclassical EBK quantization [2, 3], the distance between two neighbouring quasiangles is approximately given by 2π times the classical winding number Ω. As shown in figure 4, distances decrease monotonously with the ordering number up to the state $|15\rangle$. This trend continues smoothly from the inner regular region (a) to the chaotic region (b–d). The strong deviation for the states $|16\rangle$ and $|22\rangle$ marks the beginning and the end of the resonance region (c), where the quasiangles are almost equidistant and the states show a strong structural similarity. Beyond this resonance region, the quasiangle separations decrease up to the state $|32\rangle$, which is localized on the inner boundary of the outer regular region (e). Here, the function shows a pronounced minimum followed by a steep increase. The position of the resonance regime and the transition from the chaotic to the outer regular regime are therefore clearly visible in the quasienergy separation of the properly ordered states.

Inside the stability islands, the classical winding number decreases from $\Omega = 1.396$ to $\Omega = 1.376$ (compare with [2]) corresponding to quasiangles of 2.489–2.365, which is in agreement with the computed quantum values. In the plateau region, one finds a winding number of $\Omega = 1.332 \approx \frac{4}{3}$ from the average quasiangle distance $\Delta\Theta = 2.085$. The deviations of the quasiangle for the states $|16\rangle$ and $|22\rangle$ from the overall trend in figure 4 can be interpreted as due to the influence of the resonance. The quasiangles in the resonance region are almost equidistant.

The value of the minimum at state $|32\rangle$ with $\Delta\Theta = 1.270$ agrees well with the winding number $\Omega = 1.202$ of the corresponding flux tube [2], which once more allows an EBK quantization in the outer regular region. Further out, the quasiangle distances and winding numbers increase with approximately equal values.

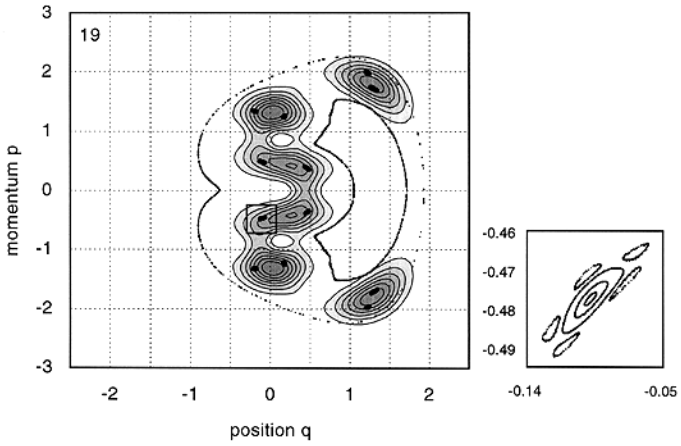

Figure 5. Husimi distribution of the resonance state $|19\rangle$. Classically, this state is supported by a chain of 12 islands marked by dots. Also shown are the boundaries of the regular region and a magnification of one of the classical islands.

4.2. Resonance states

The strong structure of the Husimi distribution of the states $|16\rangle$–$|21\rangle$ are all very similar (distinguished, however, by their increasing number of inner zeros) and show a pronounced localization on six points in phase space as shown for state $|16\rangle$ in figure 3 and $|19\rangle$ in figure 5. Semiclassically, the equidistant quasiangles correspond to the rational winding number $\frac{4}{3}$ of a classical vortex tube, which suggests a resonance phenomenon.

Analysis of the classical system reveals small stability islands embedded in the chaotic sea in the neighbourhood of the localization region of the Husimi distributions. In figure 5, a chain of 12 islands is marked by dots. Also shown are the boundaries of the regular classical region as well as a magnification of one of the islands. Because of the comparatively large value of $\bar{h}$, the Husimi distributions of state $|19\rangle$ in figure 5 does not fully resolve the 12 small islands. Six maxima of the distribution appear, which are localized in the middle of pairs of neighbouring islands extending over an area of the order of $h \approx 0.3$.

Despite the apparently uniform classical region, the resonance states $|16\rangle$–$|21\rangle$ are strongly influenced by the embedded bifurcated elliptic fixed points. These island regions originate from a flux tube with winding number $\frac{4}{3}$, which is distorted and partly destroyed, and only 12 periodic islands have survived. The quantum phase space entropy in figure 2 shows pronounced minima in these regions, i.e. quantum localization supported by classical fixed-point structures, whose area is small compared to h.

4.3. Resonance transition

In the following, the resonance transition from state $|15\rangle$ to state $|16\rangle$ is discussed in more detail. Figure 6 compares the Husimi distributions of both states. The zeros of the distributions are marked by open circles and squares, where the inner ones (circles) are taken into account for the determination of the quasienergy ordering number.

In the transition to state $|16\rangle$, a structural change of the configuration of maxima and zeros is observed. For the state $|15\rangle$, the 15 essential zeros are located in the inner low density region, which is similar in form to the classical stability island. This region is surrounded by a ridge of large values of the Husimi distribution, interrupted by six zeros

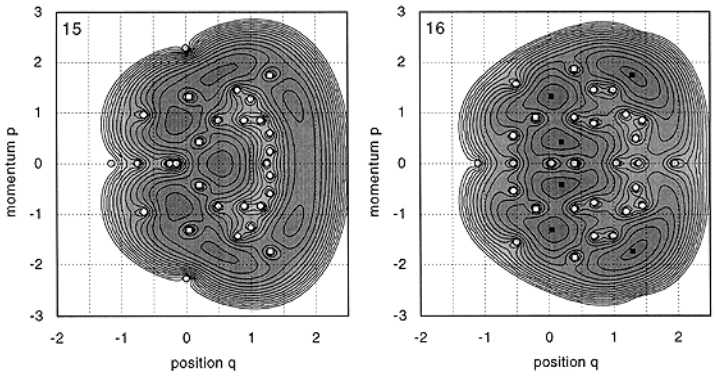

Figure 6. Resonance transition: Husimi distribution of states $|15\rangle$ and $|16\rangle$ (logarithmic scaling). The essential zeros are marked by open circles or squares. In the transition the six zeros and maxima along the ridge exchange their role.

(marked by open squares). All these six zeros are located at the remaining elliptic fixed points of the destroyed flux tube with winding number $\frac{4}{3}$ as described in section 4.2.

For the state $|16\rangle$, the ridge structure has drastically changed. The distribution shows six pronounced maxima (marked by full squares), whose positions correspond to the six zeros of the state $|15\rangle$ marked by open squares. The resonance transition interchanges the localization of low and high density, i.e. zeros and maxima, on the ridge.

Furthermore, it should be noted that the zeros marked by squares in figure 6 for state 16 are very close to the classical hyperbolic fixed points, while those of state 15 are close to the elliptic ones. The 16 'essential' zeros are located inside the regions of the hyperbolic and elliptic fixed points, i.e. within the destroyed flux tube with winding number $\frac{4}{3}$.

Finally, it should be pointed out that a related observation of a localization of the Husimi zeros on families of classical stable and unstable resonance orbits (i.e. a 'scarring' of the wavefunction) has been reported in a very recent study of a two-dimensional time-independent system [29] modelling LiCN [29].

5. Concluding remarks

As pointed out in a recent article by Dando and Monteiro [17]: 'The detailed morphology of quantum phase space for individual states when some or all classical phase space is chaotic, remains an open theoretical problem.' In the present study we have demonstrated for a one-dimensional time periodic system that the zeros of the Husimi phase space distribution carry valuable information in close connection with the underlying classical dynamics. Quite unexpected, the zeros could be used for a classification and even an ordering of the quasienergy states. However, the present classification has been made easier by the simple phase space structure and may not directly be applied to more complex situations. Additional studies for such systems are required.

Furthermore, it is demonstrated that the distribution of zeros reveals distinctive patterns in the classically chaotic or regular regions of phase space, which show a structural reorganization in characteristic (resonance) transitions. The localization of the 'resonance state' corresponds classically to a (partly destroyed) chain of elliptic/hyperbolic fixed points and classical phase space structures localized on an area small in comparison with h show a pronounced influence on the quantum states.

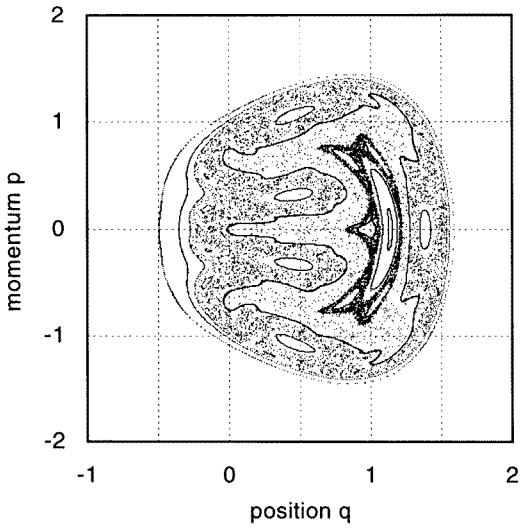

Figure 7. Classical stroboscopic Poincaré section for a driven quartic oscillator (parameters $b = 0.25$, $f = 0.5$, $\omega \approx 0.618$). Two distinct chaotic regimes are separated by a KAM torus.

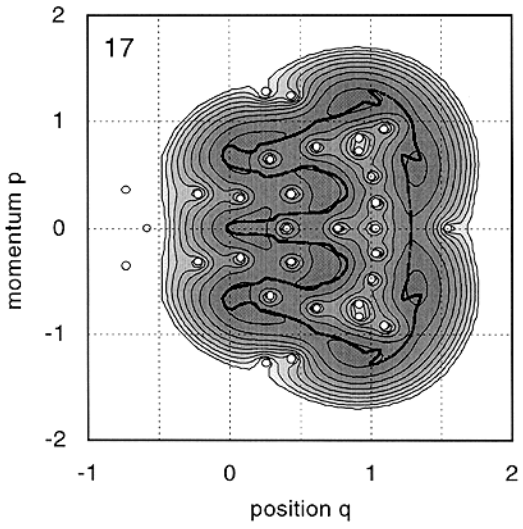

Figure 8. Husimi distribution of state $|17\rangle$ for the quartic oscillator shown in figure 7 ($\bar{h} = 0.02$). Also shown is the classical KAM torus separating the two chaotic regions.

Similar observations for different parameters of the Hamiltonian (6) support these observations. As an example, another connection between the position of the zeros of the Husimi distribution and classical phase space structures shall be briefly discussed, which demonstrate the correspondence between the position of the zeros and the classical phase space structure for the case of an intact KAM torus. Figure 7 shows a stroboscopic Poincaré section of the quartic oscillator (6) for a strongly irrational driving frequency $\omega = (\sqrt{5} - 1)/2 \approx 0.618$. In this special case we have two distinct extended chaotic regions, which are separated by a thin KAM torus with winding number 0.822 (a noble number). Classically, this KAM torus is an impenetrable obstacle for the phase space flow. In addition, one observes a cantorus inside the inner chaotic region. Figure 8 shows the Husimi distribution of a selected quasienergy state ($\bar{h} = 0.02$). This state, $|17\rangle$ as numbered by the essential zeros, localizes on the separating KAM torus (in fact, it can be quantized semiclassically by an EBK torus quantization). Because of the nondestruction of the KAM

torus for this case, the correct allocation of the zeros causes no problem.

Inside the classical KAM torus, which is also shown in the figure, we find the 17 zeros, which are used in the ordering of states. In the neighboured states $|16\rangle$ and $|18\rangle$ 16 resp. 18 zeros are found inside the KAM torus.

In summary, we have presented numerical evidence for the importance of the zeros of the Husimi function. Clearly, our discussion is quite descriptive and a deeper theoretical analysis is necessary to validate (or disprove) our findings.

Acknowledgment

This research has been supported by the Deutsche Forschungsgemeinschaft (SPP: 'Zeitabhängige Quantensysteme').

References

[1] Breuer H P and Holthaus M 1991 *Ann. Phys., NY* **211** 249
[2] Bensch F, Korsch H J, Mirbach B and Ben-Tal N 1992 *J. Phys. A: Math. Gen.* **25** 6761
[3] Mirbach B and Korsch H J 1994 *J. Phys. A: Math. Gen.* **27** 6579
[4] Gutzwilller M C 1990 *Chaos in Classical and Quantum Mechanics* (New York: Springer)
[5] Takahashi K 1989 *Prog. Theor. Phys. Suppl.* **98** 109
[6] Korsch H J and Berry M V 1981 *Physica* **3D** 627
[7] Saraceno M 1990 *Ann. Phys., NY* **199** 37
[8] Takahashi K and Saitô N 1985 *Phys. Rev. Lett.* **55** 645
[9] Ben-Tal N, Moiseyev N and Korsch H J 1992 *Phys. Rev.* A **46** 1669
[10] Lee H-W 1994 *Phys. Rev.* A **50** 2746
[11] Lin W A and Ballentine L E 1990 *Phys. Rev. Lett.* **65** 2927
Lin W A and Ballentine L E 1992 *Phys. Rev.* A **45** 3637
[12] Plata J and Gomez Llorente J M 1992 *J. Phys. A: Math. Gen.* **25** L303
[13] Dittrich T, Oelschlägel B and Hänggi P 1993 *Europhys. Lett.* **22** 5
[14] Utermann R, Dittrich T and Hänggi P 1994 *Phys. Rev.* E **49** 273
[15] Hänngi P, Utermann R and Dittrich T 1994 *Physica* **194–6B** 1013
[16] Averbuckh V, Moiseyev N, Mirbach B and Korsch H J 1995 *Z. Phys.* D **35** 247
[17] Dando P A and Montiero T S 1994 *J. Phys. B: At. Mol. Opt. Phys.* **27** 2681
[18] Dando P A, Monteiro T S, Jans W and Schweizer W 1994 *Prog. Theor. Phys. Suppl.* **116** 403
[19] Müller K and Wintgen D 1994 *J. Phys. B: At. Mol. Opt. Phys.* **27** 2693
[20] Mirbach B and Korsch H J 1995 *Phys. Rev. Lett.* **75** 362
[21] Lebœuf P and Voros A 1990 *J. Phys. A: Math. Gen.* **23** 1765
[22] Bogomolny E, Bohigas O and Lebœuf P 1992 *Phys. Rev. Lett.* **68** 2726
[23] Hannay J 1996 *J. Phys. A: Math. Gen.* **29** L101
[24] Lebœuf P 1991 *J. Phys. A: Math. Gen.* **24** 4575
[25] Cibils M B, Cuche Y, Lebœuf P and Wreszinski W F 1992 *Phys. Rev.* A **46** 4560
[26] Toda M 1992 *Physica* **59D** 121
[27] Tualle J-M and Voros A 1995 *Chaos, Solitons and Fractals* **5** 1085
[28] Prosen T 1996 *Physica* **91D** 244
[29] Arranz F J, Borondo F and Benito R M 1996 *Phys. Rev.* E **54** 2458
[30] Bargmann V 1961 *Commun. Pure Appl. Math.* **14** 187
Bargmann V 1967 *Commun. Pure Appl. Math.* **20** 1
[31] Lütkenhaus N and Barnett S M 1995 *Phys. Rev.* A **51** 3340
[32] Ben-Tal N, Moiseyev N. Fishman S, Bensch F and Korsch H J 1993 *Phys. Rev.* E **47** 1646
[33] Korsch H J and Wiescher H 1996 Quantum chaos, *Computational Physics: Selected Methods—Simple Exercises—Serious Applications* ed K H Hoffman and M Schreiber (Berlin: Springer) p 225
[34] Wiescher H 1996 *Diplomarbeit* University Kaiserslautern
[35] Moiseyev N, Korsch H J and Mirbach B 1994 *Z. Phys.* D **29** 125
[36] Norris J W 1992 *J. Lond. Math. Soc.* vol 2 **45** 97
[37] Howland J S 1992 *J. Phys. A: Math. Gen.* **25** 5177